

Analysis of *MOST* light curves of five young stars in Taurus–Auriga and Lupus 3 star-forming regions[★]

Michal Siwak,^{1,2†} Slavek M. Rucinski,¹ Jaymie M. Matthews,³ Rainer Kuschnig,^{3,4}
David B. Guenther,⁵ Anthony F. J. Moffat,⁶ Dimitar Sasselov⁷ and Werner W. Weiss⁴

¹Department of Astronomy and Astrophysics, University of Toronto, 50 St George Street, Toronto, ON M5S 3H4, Canada

²Mount Suhora Astronomical Observatory, Cracov Pedagogical University, ul. Podchorazych 2, 30-084 Krakow, Poland

³Department of Physics and Astronomy, University of British Columbia, 6224 Agricultural Road, Vancouver, BC V6T 1Z1, Canada

⁴Institut für Astronomie, Universität Wien, Türkenschanzstrasse 17, A-1180 Wien, Austria

⁵Institute for Computational Astrophysics, Department of Astronomy and Physics, Saint Marys University, Halifax, NS B3H 3C3, Canada

⁶Département de Physique, Université de Montréal, C.P. 6128, Succursale: Centre-Ville, Montréal, QC H3C 3J7, Canada

⁷Harvard–Smithsonian Center for Astrophysics, 60 Garden Street, Cambridge, MA 02138, USA

Accepted 2011 March 9. Received 2011 March 7; in original form 2011 January 20

ABSTRACT

Continuous photometric observations of five young stars obtained by the *MOST* satellite in 2009 and 2010 in the Taurus and Lupus star formation regions are presented. Using light-curve modelling under the assumption of internal invariability of spots, we obtained small values of the solar-type differential-rotation parameter ($k = 0.0005$ – 0.009) for three spotted weak-line T Tauri stars, V410 Tau, V987 Tau and Lupus 3-14; for another spotted weak-line T Tauri star (WTTS), Lupus 3-48, the data are consistent with a rigidly rotating surface ($k = 0$). Three flares of similar rise (4 min and 30 s) and decay (1 h and 45 min) times were detected in the light curve of Lupus 3-14. The brightness of the classical T Tauri star RY Tau continuously decreased over 3 weeks of its observations with a variable modulation not showing any obvious periodic signal.

Key words: stars: individual: RY Tau – stars: individual: V410 Tau – stars: individual: V987 Tau – stars: individual: Lupus 3-14 – stars: individual: Lupus 3-48 – stars: rotation.

1 INTRODUCTION

The Canadian *Microvariability and Oscillations of Stars (MOST)* satellite, designated to obtain high precision photometry of bright stars, offers a unique opportunity to achieve good-quality, continuous light curves of fainter objects (to about 11 mag) with coverage extending to dozens of days. Among other applications, such extend time monitoring permits studies of stellar surface rotation rates and of their differential characteristics as well as flares on active spotted stars (Rucinski et al. 2004; Croll et al. 2006; Walker et al. 2007; Siwak et al. 2010) In this investigation, we present recently obtained *MOST* light curves of five T Tauri (T Tau)-type stars.

The targets investigated in this paper are members of two different star-forming regions (SFRs): Three, V410 Tau, V987 Tau and RY Tau belong to the Taurus–Auriga SFR; we refer the interested reader to Skelly et al. (2010), Strassmeier & Rice (1998) and

Petrov et al. (1999) for more historical details about these stars. The two Lupus targets were discovered by the *ROSAT* satellite in the Lupus 3 SFR (Krautter et al. 1997). Although for dozens of stars in the Lupus 3 SFR Wichmann et al. (1999) obtained high-resolution spectra and determined their spectral types and projected rotational velocities $v \sin i$, the stars remained rather poorly studied, both photometrically and spectroscopically.

Four of the targets (V410 Tau, V987 Tau, Lupus 3-14, Lupus 3-48) belong to the weak-line sub-type of T Tau stars (WTTS) and appear to show very similar variations, apparently caused by large photospheric spots. For all these objects, the same assumption of differentially rotating surfaces covered by large spots can be applied. The fifth target, RY Tau, is a classical T Tau star showing significant (previously up to a few magnitudes) and irregular brightness variations described as Type III variability (Herbst, Herbst & Grossman 1994) which is most probably caused by variable absorption/extinction events due to circumstellar dust. Table 1 gives the key physical parameters of targets investigated in this paper.

The paper is organized as follows. We present details concerning data acquisition and reduction in Section 2. The methods used for light-curve analysis are described in Section 3. The results obtained for individual targets are discussed in Section 4 and then summarized in Section 5.

[★]Based on data from the *MOST* satellite, a Canadian Space Agency mission, jointly operated by Dynacon Inc., the University of Toronto Institute of Aerospace Studies and the University of British Columbia, with the assistance of the University of Vienna.

†E-mail: siwak@nac.ou.uj.edu.pl

Table 1. Physical parameters of targets.

star	Spc.	T_{eff}	$\log g$	$v \sin i$	i
V410 Tau ^a	K5	4500	4.0	74(3)	70(10)
V987 Tau ^b	G5IV	5250	3.5	78(1)	35^{+15}_{-5}
Lupus 3-14 ^c	K0Ve	5190 ^d	–	–	–
Lupus 3-48 ^e	K2	4900 ^d	–	49.0	–
RY Tau ^f	G1	5945	–	51.6	25(3)

^aSkelly et al. (2010).^bStrassmeier & Rice (1998).^cCDS.^dEstimated in this paper from the available data, based on spectral type-effective temperature calibration of Harmanec (1988).^eWichmann et al. (1999).^fPott et al. (2010).

The uncertainties, if known, are given in parentheses.

2 OBSERVATIONS AND DATA REDUCTIONS

The optical system of the *MOST* satellite consists of a Rumak–Maksutov $f/6$, 15-cm reflecting telescope. The custom broad-band filter covers the spectral range of 380–700 nm with effective wavelength falling close to the Johnson V band. The pre-launch characteristics of the mission are described by Walker et al. (2003) and the initial post-launch performance by Matthews et al. (2004).

The stars investigated in this paper were observed in the direct-imaging mode of the satellite (Walker et al. 2003). RY Tau, V410 Tau and V987 Tau were observed together, within one field, between 2009 October 19 and November 9. Lupus 3-14 and Lupus 3-48 were chosen as secondary targets in the field of the primary *MOST* target HR 5999 and were observed between 2009 April 18 and 30. Lupus 3-14 was observed during a second observing run of HR 5999 between 2010 May 3 and 25. The individual exposure times were 30 or 60 s long. In general, the targets were observed during the low stray-light orbital phases of *MOST* which lasted typically 40 min of every 103-min satellite orbit, although occasionally the data acquisition was interrupted for up to a few *MOST* orbits due to technical problems. Additionally, we removed a portion of the data for RY Tau and V410 Tau which was affected by reflections in the telescope optics caused by the Moon’s passage within $\approx 4^\circ$ – 6° .

Aperture photometry of stars was obtained using *dark-corrected* images by means of the *DAOPHOT II* package (Stetson 1987). The *dark* frames were obtained by averaging a dozen *empty-field* images specifically taken during each observing run. In the case of stars in the Taurus field, a weak correlation between the star flux and the sky background level within each *MOST* orbit, most probably caused by a small photometric non-linearity of the electronic system (see Siwak et al. 2010), was noticed and removed. No such correlations were observed for targets in the Lupus field. The light curves were also corrected by low-order polynomials for slow photometric trends determined from a few constant stars observed simultaneously with the respective targets. As a result, we obtained good quality light curves with median errors of the *mean-orbital* data points expressed in normalized flux units of 0.0015 (V987 Tau), 0.0032 (V410 Tau), 0.0014 (RY Tau), 0.0055 (Lupus 3-14) and 0.0062 (Lupus 3-48). The mean-orbital errors were used in calculating weights during the reduced and weighed χ^2 calculation. However, as we will stress later, the model parameter uncertainties are not driven by random errors, but rather by the unavoidably large ranges in assumed astrophysical parameters such as the flux level for the unspotted photosphere and – particularly – the inclination of the rotation axis.

3 LIGHT-CURVE ANALYSIS: THE METHODS

We used two different techniques for analysis of the four spotted stars and for RY Tau which showed a complex, evolving light curve:

(1) For the light curve of RY Tau, we used the Fourier transform technique for unevenly sampled data; the results are described in Section 4.5.

(2) For the four spotted stars, we used the spot model program *StarSpotz*, as described in Croll et al. (2006) and Walker et al. (2007).

Because the results for RY Tau are rather inconclusive, we concentrated on the determination of the differential rotation of the four spotted stars assuming that the dark spots are invariable in time (except for longitudinal drifts caused by differential rotation). This assumption is supported by the results of several Doppler imaging campaigns for V410 Tau and V987 Tau (see Sections 4.1 and 4.2). As it will be shown below, their global, progressive light-curve shape changes can be fully explained by differential rotation of their stellar surface. Any random, rapid or small-scale changes of the spots appear to be absent or have been averaged over the duration of the *MOST* observations.

During the light-curve modelling process, we assumed the following parameters as constant (if known, see Table 1): the rotation axis inclination i , the stellar radius R and the projected rotational velocity $v \sin i$. Assuming photospheric and spot temperatures of $T_{\text{eff}} = 4500$ K and $T_{\text{spot}} = 3600$ K (Skelly et al. 2010) for V410 Tau and $T_{\text{eff}} = 5250$ K and $T_{\text{spot}} = 3800$ K for V987 Tau (Strassmeier & Rice 1998), the *spot-to-photosphere* flux ratios $f = 0.077 \pm 0.015$ and 0.105 ± 0.015 were evaluated for the *MOST* filter bandpass by means of the *SPECTRUM* program (Gray 2001) and Kurucz’s atmosphere models (Kurucz 1993). The same value of f was assumed for all spots on a given star. Because the *MOST* magnitudes are very close to those of Johnson V ones (Siwak et al. 2010), we assumed the linear limb-darkening coefficients $u = 0.817$ (for V410 Tau) and $u = 0.737$ (for V987 Tau), calculated for the Johnson V band by Díaz-Cordovés, Claret & Giménez (1995). Due to the absence of data on $\log g$ for Lupus 3-14 and Lupus 3-48, we assumed the identical value of $f = 0.08$ and the limb darkening corresponding to their spectral types of $u = 0.737$ and 0.78; we noted that the exact value of u has a second-order effect on the predicted light curves compared with effects caused by the assumed simple circular geometry of spots. Except for V410 Tau, the unspotted magnitudes and hence the corresponding values of spot-free stellar fluxes (F_u) were not known for our targets; for this reason, we performed a grid of solutions for several fixed values of F_u (1.0, 1.1, . . . , 1.7). In Table 2, we present the results obtained for the best-fitting values of F_u .

The adjusted parameters of the model were, for each of two spots, (1) the initial moment t in $hjd_1 \equiv \text{HJD} - 245\,5100$ (for stars in the Taurus field) or $hjd_2 \equiv \text{HJD} - 245\,4900$ (for stars in the Lupus 3 field), when the spot is facing the observer, (2) the rotation period p of the spot in days, (3) the latitude ϕ of the spot in degrees and (4) its diameter r in degrees.

During the search for the solar-type differential-rotation coefficient k , the individual spot rotation periods p_j were assumed to depend on the stellar latitude ϕ_j , on the rotational period at the equator P_{eq} (in days) and on the differential-rotation parameter k through the solar-type rotation law:

$$p_j(\phi_j) = P_{\text{eq}} / (1 - k \sin^2 \phi_j), \quad (1)$$

where $j = 1, 2$ denote the individual spots.

Table 2. The light-curve models for the four WTTS, obtained for the assumed inclinations i . The ranges of the derived parameters given in parentheses correspond to the extreme possible values of i , as given in Table 1, with the exception of the targets from the Lupus 3 SFR, where we assumed $i = 60^\circ \pm 20^\circ$.

Star:	V410 Tau	V987 Tau	Lupus 3-14	Lupus 3-48
F_u	1.55 ^a	1.1 ^a	1.1 ^a	1.0 ^a
i ($^\circ$)	70 (60–80) ^a	35 (30–50) ^a	60 (40–80) ^a	60 (40–80) ^a
$v \sin i$ (km s ⁻¹)	74 ^a	78 ^a	–	49 ^a
R (R $_\odot$)	2.9 (3.2–2.8)	4.1 (4.7–3.1)	–	2.3 (3.0–2.0)
P_{eq} (d)	1.871 97 ^b	1.5215 (1.5220–1.5210) ^b	1.257 (1.259–1.256)	–
k	0.0005(1) ^b	0.0064 (0.0063–0.0066) ^b	0.009 (0.008–0.01)	–
p_1 (d)	1.873 01 ^c	1.522 06 (1.522 40–1.522 43) ^c	1.2681 (1.2683–1.2684) ^c	2.019 73 (2.019 71–2.019 64)
t_1 ($hjd_{1,2}$)	24.952 (24.950–24.970)	24.452 (24.449–24.450)	40.241 (40.241–40.260)	40.780 (40.780–40.768)
ϕ_1 ($^\circ$)	75.4 (76.0–71.6)	13.9 (11.8–22.0)	80.1 (73.2–81.7)	60.4 (41.7–72.0)
r_1 ($^\circ$)	84.8 (77.2–90.0)	13.7 (15.6–11.0)	33.4 (24.7–48.3)	13.4 (11.8–22.0)
p_2 (d)	1.872 66 ^c	1.530 52 (1.530 53–1.530 77) ^c	1.2605 (1.2596–1.2613) ^c	2.019 73 (2.019 71–2.019 64)
t_2 ($hjd_{1,2}$)	25.977 (25.982–25.974)	25.378 (25.373–25.382)	40.715 (40.722–40.714)	41.472 (41.473–41.455)
ϕ_2 ($^\circ$)	–52.3 (–48.9––58.1)	73.6 (70.2–79.5)	33.7 (13.4–40.5)	7.5 (0.4–36.8)
r_2 ($^\circ$)	44.6 (48.0–49.8)	24.1 (23.3–29.0)	15.5 (19.1–17.0)	10.5 (14.3–10.9)
$\chi^2_{\text{red,w}}$	1.3778	2.6903	0.3916 ^d	0.2391 ^d

^aAssumed as constant during modelling.

^bDetermined using the constraints given by R and $v \sin i$.

^cCalculated using equation (1).

^dSee Section 4.4 for details.

The search procedure for k in the cases of V410 Tau and V987 Tau consisted of two steps: first, for the assumed stellar radius R (in solar units) we searched for the value of P_{eq} best corresponding to the observed $v \sin i$; then in the second step, we searched for k which would return the smallest value of the reduced and weighted χ^2 . A similar procedure was applied during the Lupus 3-48 light-curve modelling, but because the values of R and i are unknown, we assumed a wide range of inclinations within $i = 60^\circ \pm 20^\circ$ and then adjusted R to match the observed value of $v \sin i$. As no parameters are known for Lupus 3-14, we limited our investigation to quantitative estimations of P_{eq} and k only.

Although formal errors of the parameters can be calculated from the search matrix returned during Markov chain Monte Carlo computations, their values turn out to be unrealistically small. We resolved this problem by considering extreme acceptable values of the inclination in driving the uncertainties in the model results – this is the parameter whose uncertainty has the strongest impact on the obtained results. Therefore in Table 2, we present the range of possible values from light-curve models obtained for the assumed lower and highest possible values of i .

4 RESULTS FOR INDIVIDUAL TARGETS

4.1 V410 Tau

Doppler tomographic studies (Joncour, Bertout & Menard 1994a; Hatzes 1995; Rice & Strassmeier 1996) and spectropolarimetric observations of V410 Tau (Skelly et al. 2010) revealed one large cold spot at high latitudes and one or a few smaller cold spots at moderate or low latitudes. From Doppler maps obtained in the time interval of 1 yr, Rice & Strassmeier (1996) derived a small value of the solar-type differential rotation of $k = 0.001$; however, the analysis of Skelly et al. (2010) indicated a rigidly rotating stellar surface for the star.

In accordance with previous results of Doppler tomographic studies, we started computations assuming two dark spots located near to the poles and separated in longitude by nearly 180° . The final spot configuration found by the model (Table 2) is in good accor-

dance with the most recent Doppler images obtained by Skelly et al. (2010). These authors obtained the rotational period of 1.871 97 d, but because at that time the star was probably considerably more uniformly spotted (as inferred from the small amplitude of the photometric variability of only 0.04 mag compared with 0.2 mag which we observed 10 months later), this value may be close to the equatorial rotational period of the star.

Assuming the above value of the photometric period as equal to P_{eq} , we obtained the observed $v \sin i = 74$ km s⁻¹ by setting R equal to 2.91 R $_\odot$. The best model resulted in a small amount of differential rotation for this star, $k = 0.0005(1)$ (Table 2). A solid-body model provided a slightly worse fit, with $\chi^2_{\text{red,w}}$ by 4 per cent higher. The computations were obtained for the unspotted flux $F_u = 1.55$, which is the average of 1.4 and 1.7, as obtained from the comparison between the most probable value of the stellar maximum brightness during the *MOST* observations ($V_{\text{max}} \approx 10.8$ mag) and the two values of unspotted magnitude (corresponding to F_u), estimated by Petrov et al. (1994) at $V_u = 10.44$ and by Grankin (1999) at $V_u = 10.236$.

Fernández et al. (2004) summarized several historical observations of flares and reported detection of nine flares during 11 d of V410 Tau monitoring in 2001 November. The flare amplitudes in the Johnson V filter were rather moderate, 0.02–0.1 mag, but one flare reached almost 1 mag. The flares did show a tendency to appear in the light-curve minimum, when the most active spotted region was directed to the observer. A careful inspection of the *MOST* light curve, obtained during the 22-d long run, did not reveal any flares larger than 0.01 mag and of similar duration to that observed by Fernández et al. (2004). We stress that our result may be affected by interruptions of *MOST* observations during the high stray-light phases, which altogether lasted about 60 per cent of the total coverage time.

4.2 V987 Tau (HDE 283572)

The pre-main-sequence nature of V987 Tau (HDE 283572), one of the brightest known WTTS, was established by Walter et al. (1987). Two Doppler imaging sessions (Joncour, Bertout & Bouvier 1994b;

Strassmeier & Rice 1998) revealed a large cold spot in the polar region.

To retain consistency with this result and to explain the systematic light-curve changes, we assumed two dark spots: one close to the pole and directed to the observer and a second at low latitudes. For all considered values of the spot-free flux F_u (see Section 3), the best model yielded almost the same value of the differential-rotation parameter k , about 0.0064. In Table 2, we present the values obtained for $F_u = 1.1$, giving the smallest value of $\chi_{\text{red,w}}^2$. According to Johns-Krull (1996), the star seems to rotate as a solid body, but with this assumption we obtained 2.5 times larger $\chi_{\text{red,w}}^2$ than for $k \neq 0$. We also note that from the *MOST* observations we obtained a value of the rotation period that is about 40 min shorter than 1.5495 d, as obtained by Strassmeier & Rice (1998).

4.3 Lupus 3-14 (RX J1605.8–3905)

In this investigation, we limited ourselves to light-curve modelling of the 2009 data only – the 2010 data show very simple, sine-like variations and contain little information about differential rotation. It is worth noting that both the 2009 and 2010 light curves showed regular trends by about 0.03 mag, occurring on a time-scale of about 20 d. As they appear to be similar to ellipsoidal variations observed in binary stars, this may suggest that Lupus 3-14 is a binary star.

As none of the stellar parameters (R , $\log g$, $v \sin i$, i) is known for Lupus 3-14, we arbitrarily assumed the inclination $i = 60$ with a very wide range of $\pm 20^\circ$, i.e. $i = 40^\circ$ – 80° . Under the assumption of a rigidly rotating stellar surface, the 2009 data gave $p_{1,2} = 1.2649$ d, but a rather poor fit, mostly due to the constantly changing shape of the light curve. Considering different values of P_{eq} and k , the best fits resulted in considerably smaller $\chi_{\text{red,w}}^2$ than in the case of the solid-body rotational model (Table 2). Two dark spots, one located near the pole, which is directed to the observer, and one at moderate latitudes, sufficed to explain the systematic light changes in great detail. The results are rather independent of F_u (although the value of $F_u = 1.1$ yielded the best fit to the data); we feel that determination of this parameter may require long-term observations, like those started by Grankin et al. (2008). As long as the exact value of F_u remains unknown, the radii r_i of the derived spots, especially of high-latitude spots (visible through the whole rotation), will remain affected due to the strong correlation between these parameters.

During the 2009 and 2010 observing runs of Lupus 3-14, *MOST* detected three flares. The outburst amplitudes of the three flares are similar to within about 10 per cent in continuum flux units, although the amplitude of the 2009 flare is slightly smaller, possibly due to the two-times longer (60-s) exposure used. From the data of the flare observed in 2009 and from the second flare observed in 2010, we estimated the rise time rate (from the continuum to maximum) at 4 min and 30 s. The decline rate of the first 2010 flare was determined to be about 1 h and 45 min, which is comparable with the orbital period of the *MOST* satellite and hence only roughly estimated. The same decline rate is most probably observed for all flares, as after each outburst event the observations gathered during the next *MOST* orbit had levels coincident with the unperturbed level.

4.4 Lupus 3-48 (RX J1608.9-3905)

Similar to the previous target, during the computations we arbitrarily assumed $i = 60^\circ \pm 20$. With this assumption, $P_{\text{eq}} = 2.02$ d and $R = 2.25 R_\odot$ reproduce the observed $v \sin i = 49 \text{ km s}^{-1}$ and (with $F_u = 1.0$) provide the smallest $\chi_{\text{red,w}}^2$. The model predicted one spot at high latitudes and a second spot close to the stellar equator. Un-

fortunately, because of the small amplitude of the light curve and relatively large errors of individual data points (probably caused by the intrinsic variability of the star and visible in the light-curve minima), we were unable to find whether the star rotates differentially; in fact, the solution with $k = 0$ suffices to explain the available data (Table 2, Fig. 1).

We note that due to the large errors of the *mean-orbital* data points of both stars from the Lupus field (caused by spurious and non-removed variability of the star flux within individual *MOST* orbits; see Section 2), the values of $\chi_{\text{red,w}}^2$ given in Table 2 are considerably smaller than unity. The respective values of $\chi_{\text{red,w}}^2$ can be brought to unity assuming median orbital errors of 0.0034 and 0.0028 for Lupus 3-14 and Lupus 3-48, respectively.

4.5 RY Tau

RY Tau is a prototype of the Type III T Tau variability (Herbst et al. 1994), which is most likely caused by large dust clouds forced to corotation by magnetic fields of the star. The occultations are irregular and colour independent (Petrov et al. 1999).

The *MOST* data indicate that the brightness of the star was falling during the run with two superimposed, short time-scale brightness decreases which occurred at $hjd_1 = 28$ and 33 (Fig. 2). Similar brightness drops appeared at $hjd_1 = 38$ and 42.5, but they were seriously influenced by the close Moon passage which caused a false symmetrical brightness dip at $hjd_1 = 39.6$ – 40.6 (this is marked by a horizontal bar in the figure). If the former brightness drops were caused by a transit of the same dusty clouds, then their orbital period would be about 9–10 d. Indeed, the Fourier spectrum of the data corrected for the continuous downward trend in brightness (by a linear fit) reveals many statistically significant peaks with that at 0.1 c/d related to such a likely periodicity (Fig. 3). However, the expected orbital periods of disc condensations are longer. For the inner disc radius (0.3 au) and the stellar mass of 1.69–2.00 M_\odot (Schegerer et al. 2008), the Keplerian orbital period is about 45 d. Such a long duration would correspond to an upper limit for the duration of the *MOST* runs and did not appear feasible for the operation reasons of the satellite. For the period of 9–10 d, the expected distance from the star would be about 22 R_\odot , a distance which is not excluded for a model of magnetic field lines enforcing corotation with the central star (Petrov 1990; Herbst et al. 1994).

5 SUMMARY

Continuous *MOST* satellite observations of four WTTS led to derivation of small values of the solar-type, differential-rotation parameter k . In three cases, k was found to be equal within the errors 0.0005(1), 0.0064(2) and 0.009(1) for V410 Tau, V987 Tau and Lupus 3-14, respectively. In all these three cases, the differential rotation provided a significantly better goodness-of-fit parameter ($\chi_{\text{red,w}}^2$) and satisfactorily explained the systematic evolution of the light curves (Fig. 1). In the fourth case of Lupus 3-48, the small amplitude of the light variations and rather large errors precluded derivation of the parameter k , but the solid-body rotation model satisfactorily explains the available data. In all our solutions, we obtained spot distributions in good accord with the results of previous Doppler imaging studies of the targets, i.e. with one large spot located near a pole (possibly a remnant of a dipole magnetic field topology from the classical T Tau phase) and a second spot at low latitudes. In this investigation, we limited ourselves to test the solar-type and the rigid body differential-rotation laws; with a more

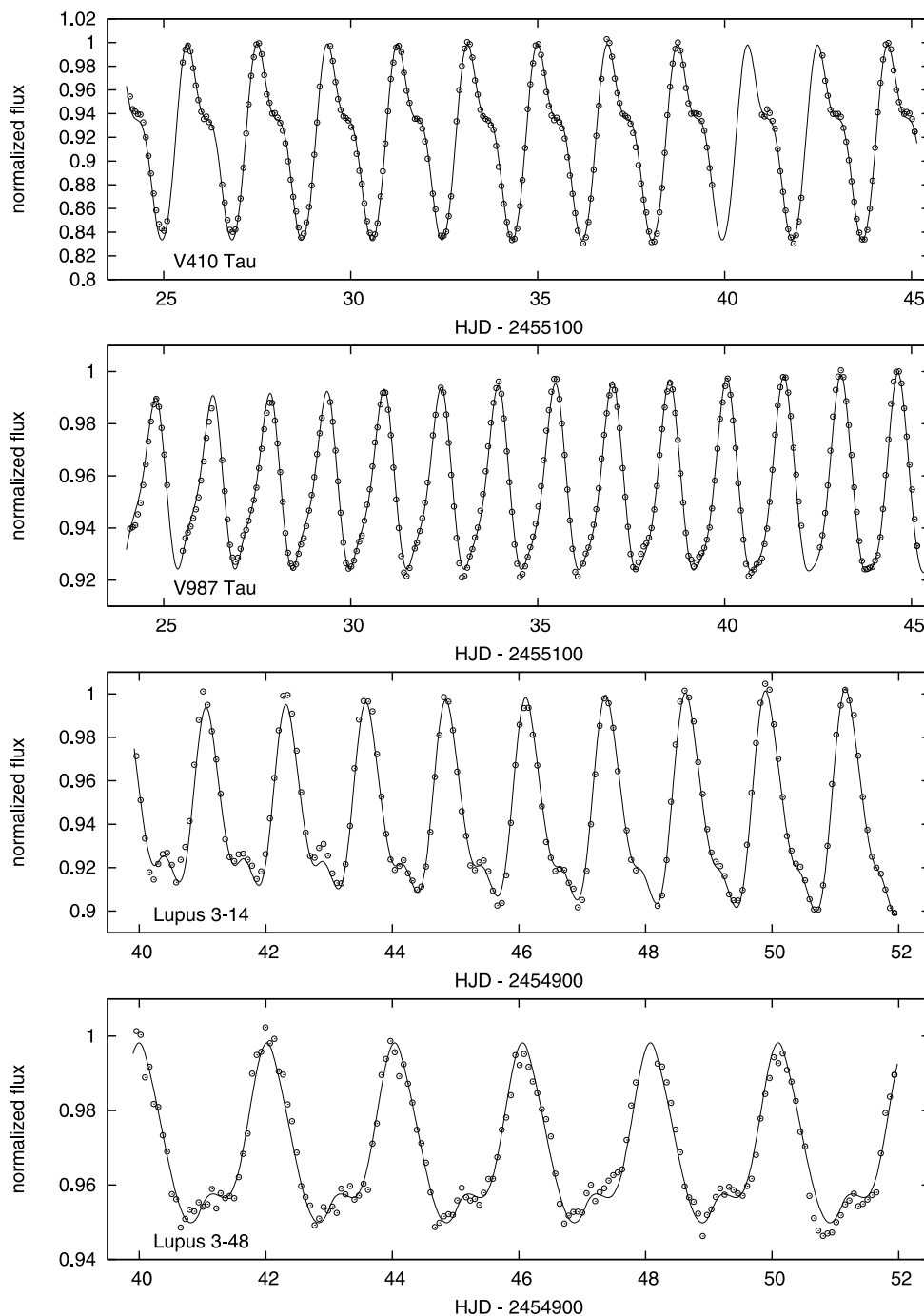


Figure 1. The comparison between the *mean-orbital MOST* data (circles) and the synthetic light curves. The flares detected in the Lupus 3-14 light curve were removed during computations. The light curves of the first three stars show systematic changes which can be interpreted as a sign of a differential rotation of their stellar surfaces, fully confirmed by the light-curve modelling. A solid-body rotation model provides a very good fit to the data of the fourth star.

reliable model of spot distribution, we plan to perform a test of the antisolar and other rotation laws.

Although all the investigated stars are known to be chromospherically active, the *MOST* data have shown flares only in the case of Lupus 3-14. For all the three large flares on this star, the rise (4 min and 30 s) and decay (1 h and 45 min) times were similar.

An even longer observing run may shed more light on the short time-scale phenomena occurring in the RY Tau light curve; the suggested orbital period (9–10 d) of small dusty clouds is only a conjectural conclusion.

ACKNOWLEDGMENTS

MS acknowledges the Canadian Space Agency Post-Doctoral position grant to SMR within the framework of the Space Science Enhancement Program. The Natural Sciences and Engineering Research Council of Canada supports the research of DBG, JMM, AFJM and SMR. Additional support for AFJM comes from FQRNT (Québec). RK is supported by the Canadian Space Agency and WWW is supported by the Austrian Space Agency and the Austrian Science Fund.

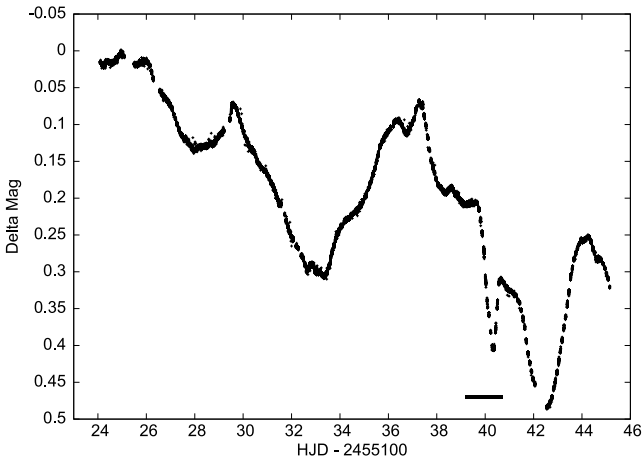


Figure 2. The light curve of RY Tau obtained by *MOST* in magnitude scale. A section of the data marked by a horizontal bar at $hjd_1 = 39.6\text{--}40.6$ was obtained during close Moon passage at an angular distance of $4^\circ\text{--}6^\circ$ from the target which has been excluded in the Fourier analysis.

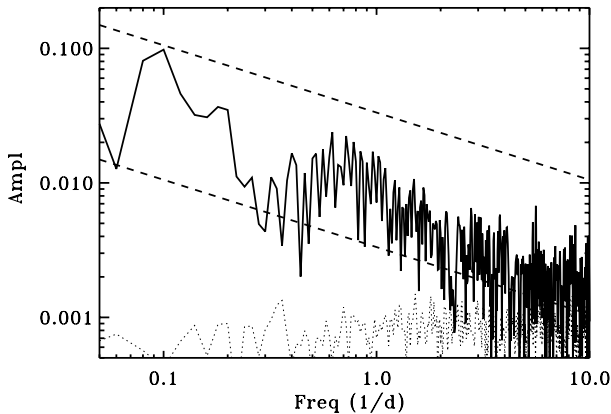


Figure 3. The Fourier transform (thick line) in log–log scale of the RY Tau light curve, detrended by a linear fit. The amplitude errors are shown as small dots.

Particular thanks are due to Mr. Bryce Croll, for preparing a special version of the StarSpotz light-curve modelling program and to the anonymous referee for useful comments and suggestions.

This research has made use of the SIMBAD data base, operated at CDS, Strasbourg, France and NASA's Astrophysics Data System (ADS) Bibliographic Services.

REFERENCES

- Croll B. et al., 2006, *ApJ*, 648, 607
 Díaz-Cordovés J., Claret A., Giménez A., 1995, *A&AS*, 110, 329
 Fernández M. et al., 2004, *A&A*, 427, 263
 Grankin K. N., 1999, *Astron. Lett.*, 25, 526
 Grankin K. N., Bouvier J., Herbst W., Melnikov S. Yu., 2008, *A&A*, 479, 827
 Gray R. O., 2001, <http://phys.appstate.edu/spectrum/spectrum.html>, Dept. Phys. Astron., Appalachian State Univ.
 Harmanec P., 1988, *Bull. Astron. Inst. Czech.*, 39, 329
 Hatzes A. P., 1995, *ApJ*, 451, 784
 Herbst W., Herbst D. K., Grossman E. J., 1994, *AJ*, 108, 1906
 Johns-Krull C. M., 1996, *A&A*, 306, 803
 Joncour I., Bertout C., Menard F., 1994a, *A&A*, 285, L25
 Joncour I., Bertout C., Bouvier J., 1994b, *A&A*, 291, L19
 Krautter J., Wichmann R., Schmitt J. H. M. M., Alcalá J. M., Neuhäuser R., Terranegra L., 1997, *A&AS*, 123, 329
 Kurucz R., 1993, *Atomic Data for Opacity Calculations*, Kurucz CD-ROM No. 1. Smithsonian Astrophys. Obser., Cambridge, MA
 Matthews J. M., Kuschnig R., Guenther D. B., Walker G. A. H., Moffat A. F. J., Rucinski S. M., Sasselov D., Weiss W. W., 2004, *Nat*, 430, 51
 Petrov P. P., 1990, *Ap&SS*, 169, 61
 Petrov P. P., Shcherbakov V. A., Berdyugina S. V., Shevchenko V. S., Grankin K. N., Melnikov S. Y., 1994, *A&AS*, 107, 9
 Petrov P. P., Zajtseva G. V., Efimov Yu S., Duemmler R., Ilyin I. V., Tuominen I., Shcherbakov V. A., 1999, *A&A*, 341, 553
 Pott J.-U., Perrin M. D., Furlan E., Ghez A. M., Herbst T. M., Metchev S., 2010, *AJ*, 710, 265
 Rice J. B., Strassmeier K. G., 1996, *A&A*, 316, 164
 Rucinski S. M. et al., 2004, *PASP*, 116, 1093
 Schegerer A. A., Wolf S., Ratzka Th., Leinert Ch., 2008, *A&A*, 478, 779
 Siwak M., Rucinski S. M., Matthews J. M., Kuschnig R., Guenther D. B., Moffat A. F. J., Sasselov D., Weiss W. W., 2010, *MNRAS*, 408, 314
 Skelly M. B., Donati J.-F., Bouvier J., Grankin K. N., Unruh Y. C., Artemenko S. A., Petrov P., 2010, *MNRAS*, 403, 159
 Stetson P. B., 1987, *PASP*, 99, 191
 Strassmeier K. G., Rice J. B., 1998, *A&A*, 339, 497
 Walker G. A. H. et al., 2003, *PASP*, 115, 1023
 Walker G. A. H. et al., 2007, *ApJ*, 659, 1611
 Walter F. M. et al., 1987, *ApJ*, 314, 297
 Wichmann R., Covino E., Alcalá J. M., Krautter J., Allain S., Hauschildt P. H., 1999, *MNRAS*, 307, 909

This paper has been typeset from a $\text{\TeX}/\text{\LaTeX}$ file prepared by the author.